J. Am. Soc. Mass Spectrom. (2011) 22:1432–1440
DOI: 10.1007/s13361-011-0155-3

RESEARCH ARTICLE

Mapping a Noncovalent Protein–Peptide Interface by Top-Down FTICR Mass Spectrometry Using Electron Capture Dissociation

David J. Clarke,[1] Euan Murray,[2] Ted Hupp,[2] C. Logan Mackay,[1] Pat R. R. Langridge-Smith[1]

[1]SIRCAMS, EastChem School of Chemistry, University of Edinburgh, West Mains Road, Edinburgh, EH9 3JJ, UK
[2]CRUK p53 Signal Transduction Group, Cell Signaling Unit, Institute of Genetics and Molecular Medicine, University of Edinburgh, Crewe Road South, Edinburgh, EH4 2XR, UK

Abstract

Noncovalent protein–ligand and protein–protein complexes are readily detected using electrospray ionization mass spectrometry (ESI MS). Furthermore, recent reports have demonstrated that careful use of electron capture dissociation (ECD) fragmentation allows covalent backbone bonds of protein complexes to be dissociated without disruption of noncovalent protein–ligand interactions. In this way the site of protein–ligand interfaces can be identified. To date, protein–ligand complexes, which have proven tractable to this technique, have been mediated by ionic electrostatic interactions, i.e., ion pair interactions or salt bridging. Here we extend this methodology by applying ECD to study a protein–peptide complex that contains no electrostatics interactions. We analyzed the complex between the 21 kDa p53-inhibitor protein anterior gradient-2 and its hexapeptide binding ligand (PTTIYY). ECD fragmentation of the 1:1 complex occurs with retention of protein–peptide binding and analysis of the resulting fragments allows the binding interface to be localized to a C-terminal region between residues 109 and 175. These finding are supported by a solution-phase competition assay, which implicates the region between residues 108 and 122 within AGR2 as the PTTIYY binding interface. Our study expands previous findings by demonstrating that top-down ECD mass spectrometry can be used to determine directly the sites of peptide–protein interfaces. This highlights the growing potential of using ECD and related top-down fragmentation techniques for interrogation of protein–protein interfaces.

Key words: FTICR, Electron capture dissociation, Noncovalent interactions, Top-down fragmentation

Introduction

Electrospray ionization mass spectrometry (ESI MS) is now a well established technique for characterizing the noncovalent interactions of proteins [1–5]. By careful control of experimental conditions, a protein can be ionized without disruption of weak noncovalent protein–ligand interactions. The resulting molecular mass measurements of the complex provide direct evidence for the stoichiometry of protein–ligand or protein–protein binding. The technique has been successfully applied to protein–-ligand interactions [6, 7], as well as analysis of intact protein complexes [8–12]. In addition, several methods have been reported to determine relative and absolute dissociation constants for specific

Electronic supplementary material The online version of this article (doi:10.1007/s13361-011-0155-3) contains supplementary material, which is available to authorized users.

Correspondence to: Pat R. R. Langridge-Smith; *e-mail:* prrls@ed.ac.uk

Received: 11 January 2011
Revised: 13 April 2011
Accepted: 15 April 2011
Published online: 11 May 2011

protein–ligand interactions [13–15]. However, deducing the precise site of noncovalent ligand binding using mass spectrometry has proved more challenging. Tandem mass spectrometry (MS/MS) is commonly used to infer sequence information about a polypeptide chain and MS/MS of intact proteins, a process known as top-down MS, has proven very successful in the analysis of covalent protein modifications [16–19]. However, when applying top-down fragmentation methodology to noncovalent protein–ligand interactions, dissociation of the complex generally occurs before fragmentation of the protein. Thus, information concerning the location of the protein-ligand interface is lost before the protein's primary structure is determined.

Interestingly, in recent years it has been demonstrated that specific fragmentation processes, which occur via nonergodic pathways, have potential for top-down analysis of protein–ligand complexes. Most successful has been the use of electron capture dissociation (ECD) [20–22], which has been shown to preferentially cleave the protein backbone without disruption of weaker, noncovalent interactions [23]. To date, ECD has been successfully used to determine the binding site of several noncovalent protein–ligand complexes [24–26]. Interestingly, all the examples reported have been protein–ligand interactions, which are primarily mediated by permanent electrostatic interactions, ion pair interactions, or salt bridges; complexes studied include α-synuclein/spermine and adenylate kinase/ATP. Indeed, it has been suggested that the intrinsic stability of these ionic interactions in the gas-phase is crucial for successful retention of the noncovalent interaction during the ECD process [25, 27]. However, hydrophobic protein–ligand interactions can be preserved in the gas phase, such as those between the protein β-lactoglobulin and a series of fatty acid ligands [28]. It is also well documented that a protein's hydrogen bonding network can be retained during MS analysis. Furthermore, early ECD studies by Haselmann et al., studying the complex between vancomycin to the tripeptide AcN-KAA-$CONH_2$, demonstrated that it is also possible to retain the complex's hydrogen-bonding network whilst cleaving the amide backbone with ECD [23]. The retention of hydrogen-bonding during ECD backbone cleavage has also been implicated in the low efficiency of fragmentation in larger proteins by ECD, a phenomenon that can be overcome by using activated ion AI-ECD [29–31]. These observations suggest protein–ligand ionic electrostatic interactions are not a prerequisite for successful interface mapping by ECD.

Here we demonstrate the ability of top-down ECD fragmentation to reveal the binding site of a noncovalent protein–peptide interaction that is not mediated by ionic interactions. Anterior gradient-2 (AGR2) is a 21 kDa protein, expressed in vertebrates, which is associated with several biological pathways [32, 33]. Most notably, AGR2 has been implicated in hormone-dependent breast cancers and in predicting poor prognosis in prostrate cancers [34–37]. Mechanistically, AGR2 has been shown to be a potent inhibitor of the important tumor suppressor protein p53 [38]. Therefore AGR2 is an attractive anti-cancer drug target [39]. Recent attempt have highlighted a hexapeptide PTTIYY as a potential AGR2 inhibitor, and it has been demonstrated that this peptide can stimulate p53 function in vivo [40]. The nature of the noncovalent bonding at the AGR2–peptide interface is not fully understood. However, as the hexapeptide is uncharged at physiologic pH, it is clear that permanent electrostatic interactions are not involved. Therefore, hydrogen bonding and/or hydrophobic interactions predominate. By analyzing the AGR2-PTTIYY complex using native ESI mass spectrometry, we show here that the complex exists in 1:1 stoichiometry. We demonstrate that the protein–peptide complex is stable to ECD, and by careful control of experimental conditions we have been able to achieve top-down fragmentation of the complex *without* ligand dissociation. This allowed us to map the binding interface to between residues 109 and 175 on AGR2. This assignment is supported by solution-phase peptide competition ELISA assays, which implicate the region of AGR2 between residues 108 and 122 as interacting with PTTIYY.

Experimental

Sample Preparation

Histidine tagged AGR2 protein was produced recombinantly in *E. coli*. Briefly, 'mature' human AGR2 (AGR2 lacking the first 20 N-terminal amino acids, encoding a cleavable signal peptide) was cloned into Gateway pDEST17 vector, expressed in *E. coli*, and recombinant protein was subsequently purified using Ni-NTA agarose beads. Prior to MS analysis, protein samples were buffer-exchanged into 50 mM NH_4OAc, pH 7.0 using PD-Miditrap Column G25 (GE Healthcare), and protein concentration was adjusted to 10 μM. PTTIYY peptide was produced by Clonestar Peptide Services, Brno, Czech Republic. The peptide was stored at a concentration of 10 mM in dimethyl sulfoxide (DMSO) and diluted as required in 50 mM NH_4OAc.

FTICR Mass Spectrometry

Mass spectrometry data was acquired on an apex-ultra Qh FTICR mass spectrometer equipped with a 12 Tesla superconducting magnet (Bruker Daltonics). Nano-ESI was performed using a NamoMate running in infusion mode and equipped with a HD_A_0 ESI chip (Advion Biosciences). Desolvated ions were transmitted to a 6 cm Infinity cell penning trap. Trapped ions were excited (frequency chirp 48–500 kHz at 100 steps of 25 μs) and detected between *m/z* 600 and 3000 for 0.5 s to yield a broadband 512 K time-domain transient. Typically, each spectrum was the sum of 50 acquisitions. The mass spectra were externally calibrated using ES tuning mix

(Agilent) and analyzed using DataAnalysis software (Bruker Daltonics).

Determination of AGR2-PTTIYY Dissociation Constant by Mass Spectrometry

The dissociation constant for the protein–peptide complex was calculated using a method described by Sannes-Lowery et al. [13]. Briefly, AGR2 (10 μM) was incubated with varying concentrations of PTTIYY aptamer (0, 5, 10, 15, 20, 25, 30, 40, 50, 75 μM) at room temperature for 30 min. The resulting complexes were then analyzed by native mass spectrometry using nESI-FTICR MS.

In order to calculate the relative concentrations of apo-AGR2 and AGR2-PTTIYY complex in each spectrum, a variation on our previously published method was used [41]. Using DataAnalysis software (Bruker Daltonics), each spectrum was background-subtracted. In order to account for all peaks within an isotope cluster, the data was then smoothed using a Gauss algorithm and a window of 0.2 *m/z*. Within this smoothed spectrum, the areas under all charge states were calculated for each species using DataAnalysis software. In order to account for the linear relationship between FTMS detector response and ion charge, these calculated areas were divided by their respective charge states. The resulting charge-normalized areas were combined to give the total area for both the apo-AGR2 and AGR2-PTTIYY complex. The relative ratios of these areas were used for quantitation. The results for each time-point were an average of the processed data from the three recorded acquisitions. This lengthy data handling procedure was automated using specifically written software, produced in-house using the Labview visual programming platform (National Instruments, Austin, TX, USA). Finally, a plot of ($[L]_i$ – [PL]) versus [PL]/[P] was produced; where [P] is the concentration of apo-AGR2, [PL] is the concentration of AGR2-PTTIYY complex, and $[L]_i$ is the initial concentration

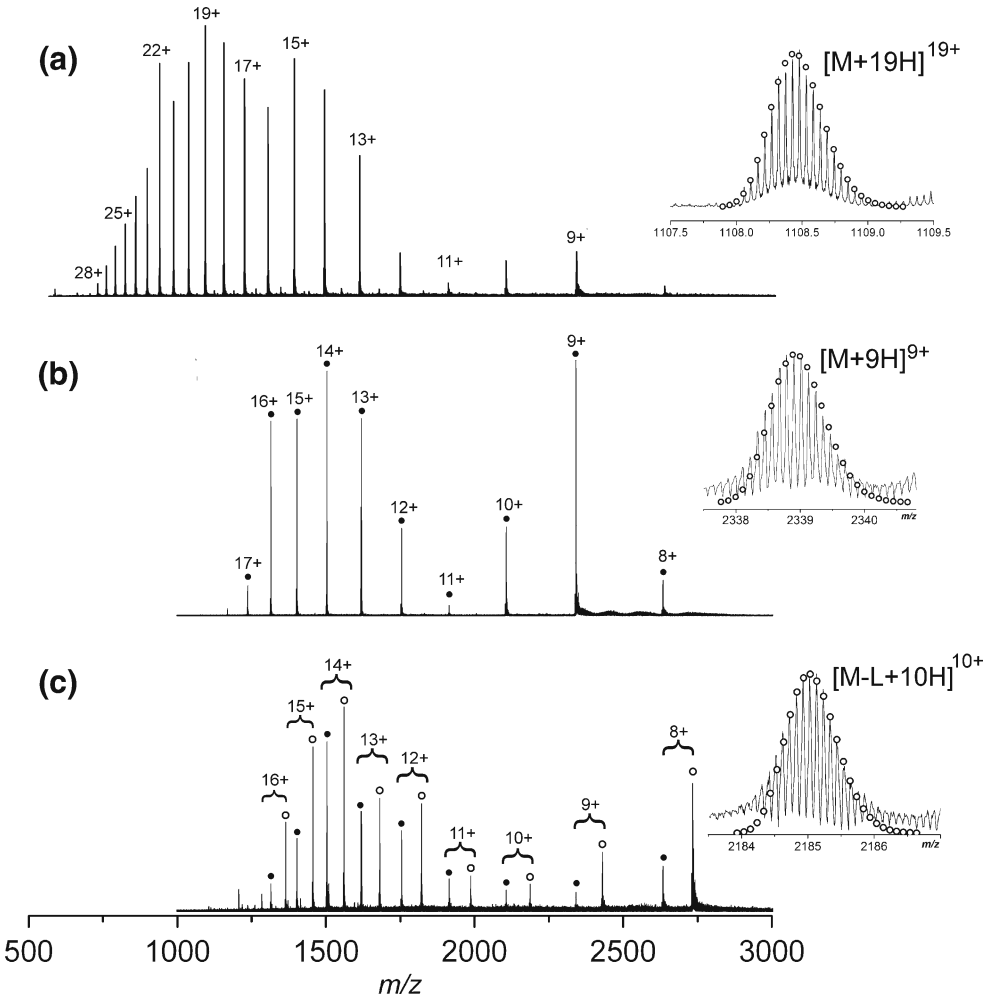

Figure 1. FTICR mass spectra of AGR2. **(a)** MS acquired under denaturing conditions in 50:50:1 MeOH:H_2O: HCOOH. **(b)** MS acquired under native conditions in 50 mM NH_4OAc, pH 7.0. **(c)** AGR2-PTTIYY complex acquired under native conditions in 50 mM NH_4OAc, pH 7.0. Charge states for various species are given. Insert: isotopic distribution of specific charge state for each spectrum. The observed isotopic distribution was consistent with the predicted elemental formula, which overlays the experimental data as a scatterplot (AGR2 theoretical elemental formula - $[C_{944}H_{1505}N_{258}O_{277}S_5]^{19+}$ and $[C_{944}H_{1495}N_{258}O_{277}S_5]^{9+}$; AGR2-PTTIYY complex - $[C_{983}H_{1550}N_{264}O_{289}S_5]^{10+}$)

of PTTIYY. The gradient of the resulting straight line, K_d^{-1}, was calculated by linear regression.

Top-Down Fragmentation

Top-down fragmentation was performed on the 12T Qh FTICR. First, a native mass spectrum was tuned for a specific charge state by varying funnel and skimmer voltages within the source optics. A specific ion species was then isolated using the mass resolving quadrupole, and MS/MS was performed using collision induced dissociation (CID) or electron capture dissociation (ECD). For CID, the collision voltage was typically set between 20 and 35V. For ECD, 1.8 A was applied to the dispenser cathode filament (Heatwave Technologies), 20 V to the lens, 0.8 V to the bias, and a pulse of between 5 and 14 ms was employed. Fragmentation data was the sum of 250–750 acquisitions, and data analyses were performed using DataAnalysis (Bruker Daltonics). The SNAP 2.0 algorithm was used for automated peak picking. The resulting top-down fragment mass lists were searched against the primary sequence of AGR2 using BioTools 3.0 (Bruker Daltonics) and Prosight-PTM software packages [42]. Mass error tolerances were set for all searches at 15 ppm.

Isotopic Fitting

Isotope distributions of specific charge states were predicted using IsotopePattern software (Bruker Daltonics) from theoretical empirical formulae. These were overlaid upon the recorded experimental data as scatter plots, with the theoretical apex of each isotope peak designated by a circle.

Peptide-Competition Assay

All peptides were acquired from Mimotopes (Clayton, Victoria, Australia) and resuspended in DMSO at 5 mg/mL. The wells of an enzyme-linked immunosorbent assay (ELISA) plate were coated with 50 µL streptavidin (2 mg/mL) overnight at 37 °C. The following day, wells were washed four times with 200 µL of PBST (PBS + 0.5% [vol/vol] Tween-20), 50 µL of AGR2 binding peptide A4:biotin-SGSG-HLPTTIYYGPPG [43] (0.1 mg/mL) was added for 1 h at room temperature, washed six times with 200 µL of phosphate buffered saline with Tween 20 (PBST), and blocked with 200 µL of 3% BSA in PBST for 1 h. Histidine tagged AGR2 (100 ng) was added to each well along with peptides 1–16 spanning the AGR2 protein sequence (5 µg) in 50 µL blocking buffer per well and incubated at room temperature for 1 h. Wells were then washed six times with PBST and probed for the presences of AGR2 using polyclonal AGR2 antibody (Moravian Biotechnology, Brno, Czech Republic) diluted 1:2000 in blocking buffer. The reaction was detected using swine-anti rabbit horseradish peroxidase (HRP) monoclonal antibody diluted 1:2000, developed using ECL and read using Fluoroscan Ascent FL.

Results and Discussion

Mass Spectrometry of Denatured AGR2

We first analyzed AGR2 protein under denaturing conditions (50:50:0.1 MeOH, H_2O, HCOOH) using FTICR MS. The resulting mass spectrum displayed a wide charge state distribution ranging from $[M + 28H]^{28+}$ to $[M + 9H]^{9+}$, and centred around the $[M + 19H]^{19+}$ species (Figure 1a). The isotopic distributions of all the observed charge states were consistent within 5 ppm of the predicted elemental formula of AGR2 (neutral elemental formula - $C_{944}H_{1486}N_{258}O_{277}S_5$; Figure 1a, insert).

Native Mass Spectrometry of AGR2 and the AGR2-PTTIYY Complex

Native nESI-FTICR mass spectra of AGR2 protein at pH 7.2 revealed a bimodal charge state distribution, with two distributions centered around $[M + 14H]^{14+}$ and $[M + 9H]^{9+}$ (Figure 1b). This observed phenomenon is characteristic of a protein, which exists in solution as two conformers at equilibrium [44–46]. The first conformer, a compact structure, gives rise to the charge states centered around $[M + 9H]^{9+}$ in the spectrum, and a second partially disordered conformer, which contributes to produce the

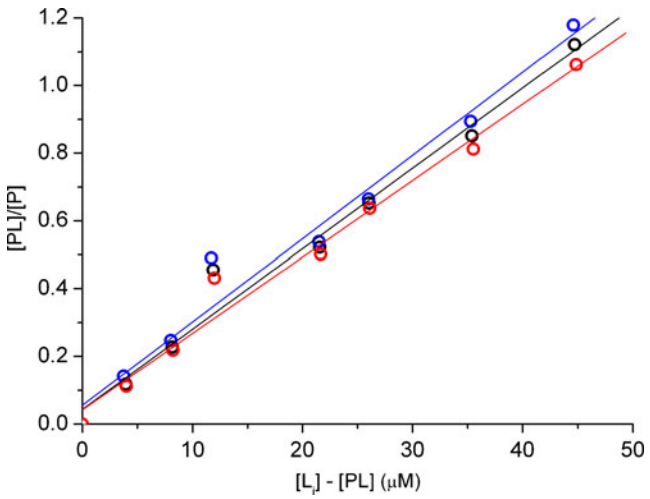

Figure 2. Determination of the dissociation constant for the AGR2-PTTIYY complex. ESI-FTICR MS titration of AGR2 (10 µM) with various concentrations of PTTIYY. Relative quantitation and calculation of equilibrium constant are described in the Experimental section. Plot of initial concentration of PTTIYY minus concentration of complex ([L_i]-[PL], x-axis) versus concentration of complex divided by concentration of free AGR2 ([PL]/[P], y-axis). The resulting straight line has a gradient of K_d^{-1}. Plots result from analysis of all observed charge states (black line, resulting K_d=42.1± 2.9 µM). Analysis of charge states +8 to +10 representing the compact AGR2 conformer (blue line, resulting K_d=40.65± 2.6 µM). Analysis of charge states +11 to +17 representing the partially disordered AGR2 conformer (red line, resulting K_d=44.3±3.4 µM)

charge states centred around the $[M + 14H]^{14+}$ species. Interestingly, this partially disordered species displays a distribution with significantly less average charge carriers than fully denatured AGR2, suggesting that this conformer exhibits some distinct solution structure.

Upon addition of the PTTIYY ligand (10 μM AGR2, 50 μM PTTIYY), native MS revealed a 1:1 AGR2-PTTIYY complex (Figure 1c). The charge state distribution of the AGR2-PTTIYY complex is similar to apo-AGR2, and again displays bimodal character. The isotope distributions of all charge states in the spectrum were consistent with the elemental formula of AGR2 in complex with a single PTTIYY ligand (neutral elemental formula - $C_{983}H_{1540}N_{264}O_{289}S_5$; Figure 1c, insert).

The peptide PTTIYY has previously been shown to compete for AGR2 binding with a labeled PTTIYY analogue (peptide A4 - biotin-SGSG-HLPTTIYYGPPG), which suggests binding occurs in a specific manner [40, 43].

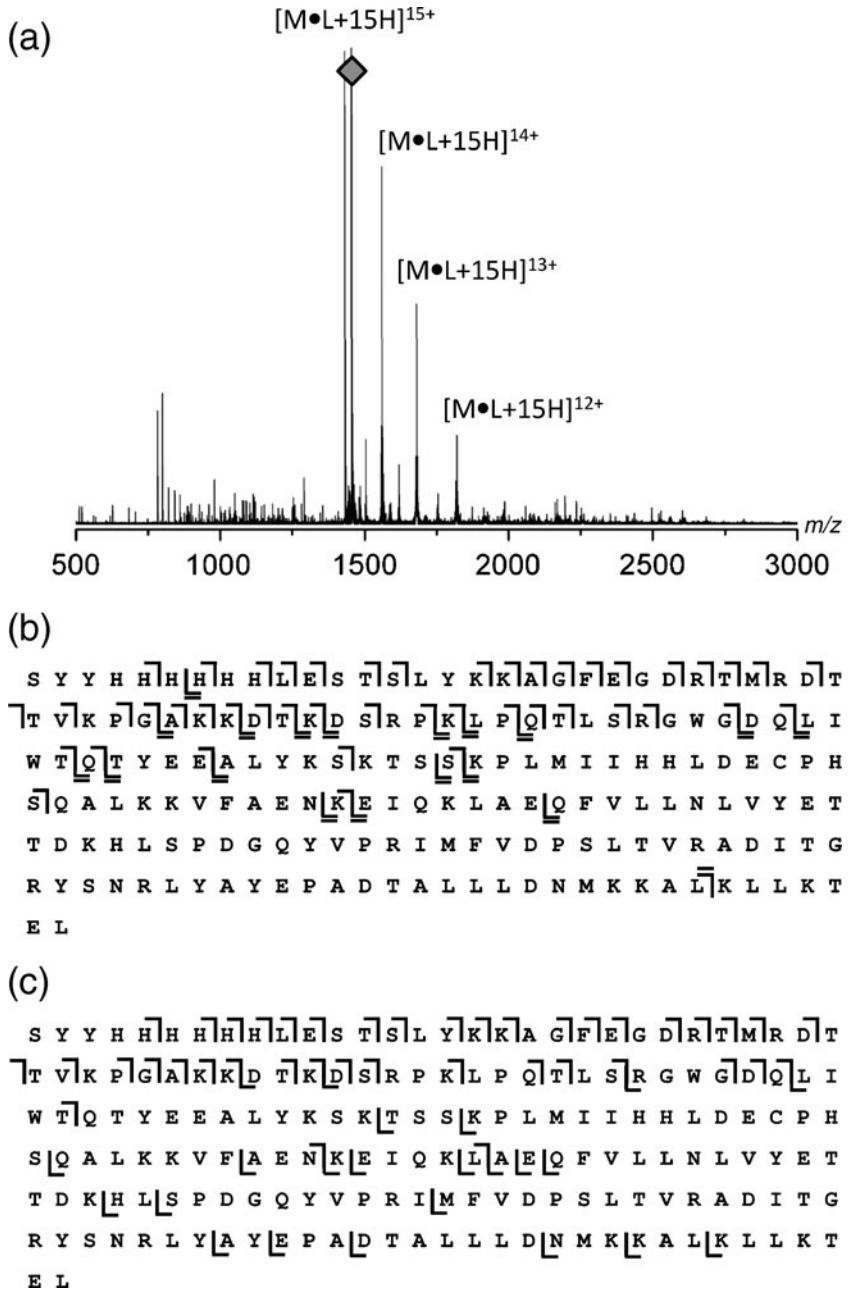

Figure 3. Top-down ECD analysis of the 15+ charge state of the AGR2:PTTIYY complex (*m/z* 1456). **(a)** Broadband ECD spectrum. Charge reduction predominates. However, backbone fragmentation is also observed. **(b)** ECD fragmentation map of the $[AGR2\text{-}PTTIYY + 15H]^{15+}$ species. Fragments which retain PTTIYY ligand binding are marked by a double tick. **(c)** ECD fragmentation map of the $[apo\text{-}AGR2 + 15H]^{15+}$ species, shown for comparison. A full list of assigned fragments is included in Tables S1 and S2

IC_{50} calculations from these experiments resulted in a value of 45.8±9.1 μM for PTTIYY competition. To complement these published findings, the dissociation constant for the protein–peptide complex was calculated from ESI-FTICR MS titrations. AGR2 was equilibrated with varying concentration of PTTIYY before analysis by native ESI-MS. A relative-ratio quantitation calculation was performed for each spectrum taking into account all observed charge states and these values were used to calculate absolute concentrations of apo- and holo-AGR2 at various ligand concentration. A plot of $[L]_i - [PL]$ versus $[PL]/[P]$ was produced, the gradient of which was used to calculate a K_d (Figure 2, see the Experimental section). The resulting value obtained for K_d of the complex between PTTIYY and AGR2 was 42.1±2.9 μM, which was in good agreement with earlier findings. This suggests that the characteristics of solution-phase binding between AGR2-PTTIYY are preserved upon transition into the gas phase.

By independently analysing the relative-ratio of the apo- and holo-peaks from the two distinct charge state distributions, individual dissociation constants were determined for both conformers of AGR2 (Figure 2, black). Handling the data in this way reveals that both conformers of AGR2 display similar dissociation constants for PTTIYY binding. Analyzing the relative ratios of the apo- and holo-AGR2 species carrying a charge of +8, +9, and +10 yields a K_d value of 40.7±2.6 μM for the interaction between the compact conformer of AGR2 and PTTIYY (Figure 2, blue). Analysis of charge states +16 to +11 yields a similar dissociation constant of 44.3±3.4 μM for the partially disordered conformer (Figure 2, red). Therefore, the structural differences between the two conformers seem to have little effect on each conformer's binding affinity for the PTTIYY ligand. Thus, our observations suggest that any disordering of the protein structure in the partially disordered conformer takes place distant from the peptide binding site.

Top-Down Fragmentation of the AGR2-PTTIYY Complex

Specific charge-states of the AGR2-PTTIYY complex were individually isolated and top-down CAD MS/MS was performed in the front end of the Qh FTICR instrument, before the ICR cell. Irrespective of the charge state isolated ($[M{\cdot}PTTIYY + 9H]^{9+}$ or $[M{\cdot}PTTIYY + 14H]^{14+}$) CAD of the noncovalent complex resulted in facile dissociation of the peptide and no information concerning the binding interface could be discerned.

In contrast, ECD MS/MS proceeded via a nondissociative pathway, retaining peptide binding. ECD was first performed on the $[M{\cdot}PTTIYY + 9H]^{9+}$ charge state of the AGR2-PTTIYY complex. Electron capture of this species was inefficient, occurring without backbone dissociation, and produced two charge reduced species, $[M{\cdot}PTTIYY + 9H]^{8+}$ and $[M{\cdot}PTTIYY + 9H]^{7+}$. Electron capture cross-section is known to increase quadratically with increasing charge, and the inability of low charge state protein ions to undergo successful ECD fragmentation is well documented [21]. Furthermore, the presence of intramolecular hydrogen bonding, such as in secondary structure elements, is thought to lower ECD fragmentation efficiency [29]. As native MS aims to retain such interactions in the gas-phase and, at the same time, results in low charge state distributions, ECD of a native protein often generates dramatically less sequence-bearing product ions than similar experiments done under denaturing conditions. These two factors have recently been highlighted in experiments by Breuker et al. [47], and by the documented use of charge-promoting agents (supercharging reagents) to increase multiple charge upon native proteins, the isolation and fragmentation of which is significantly more effective [26, 48, 49].

Next, therefore, a higher charge state of the PTTIYY-AGR2 complex (which results from the partially ordered protein conformer) was interrogated. The source optics were tuned for efficient isolation and ECD of the $[M{\cdot}PTTIYY + 15H]^{15+}$ species (*m/z* 1457). Electron capture and charge reduction without dissociation of the protein–peptide complex predominated (producing $[M\text{-}PTTIYY + 15H]^{14+}$, $[M\text{-}PTTIYY + 15H]^{13+}$, and $[M\text{-}PTTIYY + 15H]^{12+}$) (Figure 3a). In addition, extensive backbone fragmentation was also observed. Analysis of these fragments allowed the assignment of 62 unique product ions, within a mass accuracy of 15 ppm (Figure 3b). These product ions resulted from cleavage of 48 amide bonds, representing total sequence coverage of 26%. Interestingly, the majority of these fragments resulted from cleavage within the N-terminal half of the protein. Sequence coverage from Ser1 to Ser91 was 48%, compared with 4% in the region Gln92 to Leu182 (constituting only four cleavages). In

Table 1. Amino Acid Sequences of AGR2 Spanning Peptides. Each Peptide also Includes a Biotin-SGSG N-terminal Tag

Peptide	Sequence	Region (aa)[a]
P1	*LLVALSYTLA*RDTTV[b]	18–32
P2	RDTTVKPGAKKDTKD	28–42
P3	KDTKDSRPKLPQTLS	38–52
P4	PQTLSRGWGDQLIWT	48–62
P5	QLIWTQTYEEALYKS	58–72
P6	ALYKSKTSNKPLMII	68–82
P7	PLMIIHHLDECPHSQ	78–92
P8	CPHSQALKKVFAENK	88–102
P9	FAENKEIQKLAEQFV	98–112
P10	AEQFVLLNLVYETTD	108–122
P11	YETTDKHLSPDGQYV	118–132
P12	DGQYVPRIMFVDPSL	128–142
P13	VDPSLTVRADITGRY	138–152
P14	ITGRYSNRLYAYEPA	148–162
P15	AYEPADTALLLDNMK	158–172
P16	LDNMKKALKLLKTEL	168–182

[a] Region (aa) indicates the region of aa sequence of AGR2 covered by each peptide; aa numbering relates to recombinant histidine-tagged AGR2 used in this study.
[b] The P1 also peptide includes 10 aa derived from the N-terminal signal sequence of immature AGR2 (highlighted in italics).

contrast, ECD of the same charge state of apo-AGR2 under identical experimental conditions ($[M + 15H]^{15+}$ species, *m/z* 1404) resulted in similar sequence coverage in the N-terminal region (44%). However, 17 cleavages in the C-terminal region of the apo-protein were observed, 18% sequence coverage in this region (Figure 3c). Thus, ligand binding inhibits ECD fragmentation of the C-terminal region of AGR2, and our observations suggest that this region of the protein may be sterically blocked from electron capture and/or dissociation upon ligand binding. In the ECD spectrum of holo-AGR2, 18 of the observed fragments retained peptide binding (+PTTIYY empirical formula $C_{39}H_{55}N_7O_{11}$, monoisotopic mass 797.39 Da; Figure S1). Eleven of these ions are high molecular weight $z^{\bullet}$-ions, and 6 are high molecular weight z'-ions (for ECD notion see Ref. [22]). These range from $z^{\bullet}_{176+PTTIYY}$ (cleavage after His6) to $z^{\bullet}_{73+PTTIYY}$ (cleavage after Glu109). Indeed, these are the only *z* ions observed in the ECD spectrum of the [M-PTTIYY +

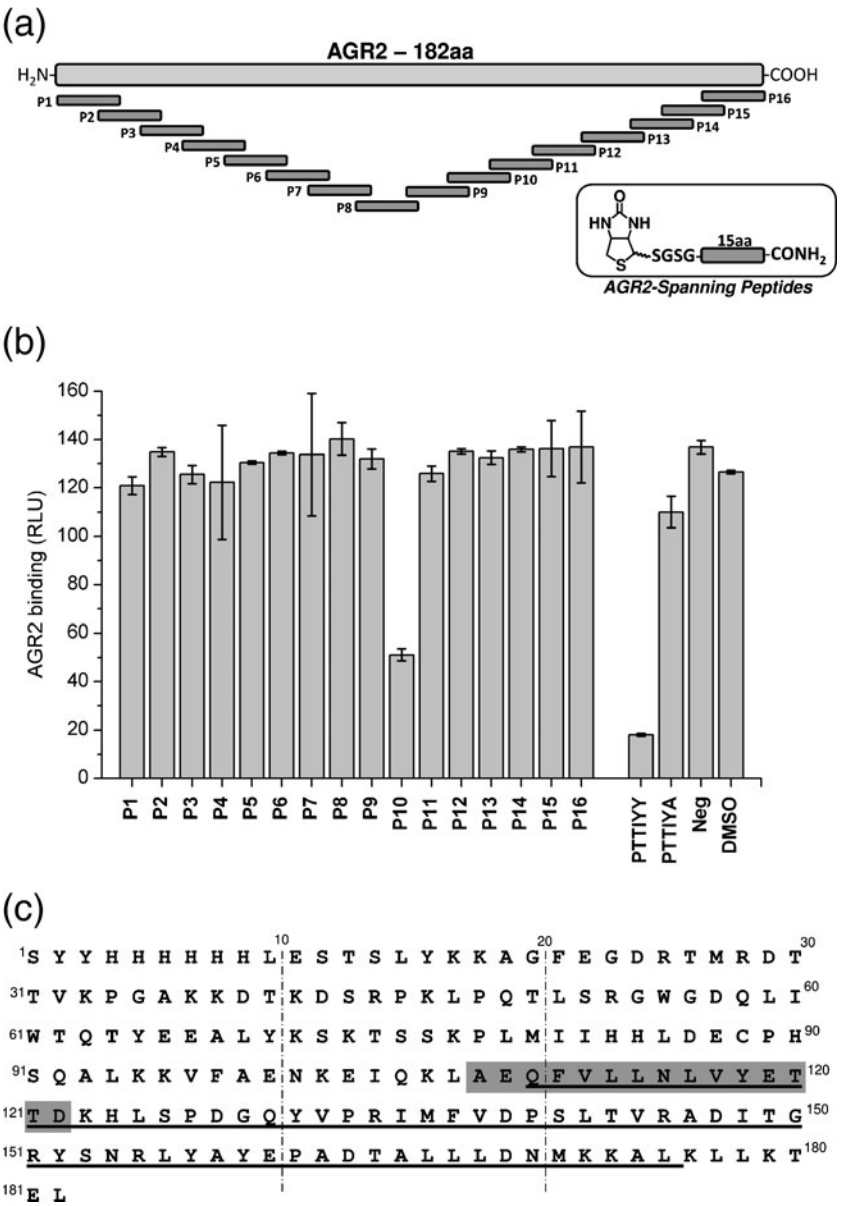

Figure 4. Analysis of AGR2-PTTIYY binding by solution peptide-competition ELISA assay. AGR2 peptide 10 blocks AGR2 protein binding to PTTIYY containing peptide. **(a)** An AGR2 peptide library was synthesized spanning the AGR2 protein sequence, each peptide is 15AA with a 5AA overlap. **(b)** AGR2 protein is captured in an ELISA by AGR2 binding peptide A4: HLPTTIYYGPPG, binding is measured as relative luminescence units (RLU); binding is blocked when carried out in the presence of peptide 10. Controls using PTTIYY ligand, the lower affinity PTTIYA, and negative controls are included. **(c)** AGR2 protein sequence indicating site of PTTIYY binding; the region of AGR2 implicated in ligand binding as deduced by ECD fragmentation is underlined; the region of AGR2 implicated in peptide binding as deduced by solution competition assay is highlighted in gray

15H]$^{15+}$ species. Only one *c* ion was observed which retains peptide binding, $c'_{175+PTTIYY}$, this results from cleavage of Leu175. No *c* ions were observed in the region of the protein from Ser91-Leu175. Taken together, these fragmentation results indicate that the protein–peptide binding interface is located in the C-terminal region of the protein, between Glu109 and Leu175.

It is interesting to note that over 75% of all observed ECD fragments of the [M + 15H]$^{15+}$ charge state of both apo-AGR2 and PTTIYY-AGR2 resulted from cleavages in the first third of the protein sequence (the N-terminal region between Ser1-Trp61). This comprehensive sequence coverage may indicate an absence of secondary structure (i.e., structural disorder) in this region of the protein. In contrast, the relatively few fragments that arise from cleavage throughout the C-terminus of the protein suggest significant structure is present in this region. Thus, this observation supports our assignment of this charge state of AGR2 as a partially disordered conformer.

Solution-Phase Analysis of the AGR2-PTTIYY Linear Binding Domain by Peptide-Competition ELISA Assay

Unfortunately, there is currently very little information on the structure of AGR2 or the location of the AGR2-PTTIYY binding interface. Therefore, in order to validate our top-down fragmentation study, the binding of AGR2-PTTIYY was investigated using a peptide-competition ELISA assay. Peptides (15 amino acid in length, Table 1) spanning the amino acid sequence of AGR2 were assayed for there ability to compete with full-length AGR2 for binding to a tagged PTTIYY peptide (peptide A4 - Biotin-SGSG-HLPTTIYYGPPG) (Figure 4a). Peptides 1–16 were individually assayed by adding each peptide concurrently with full length AGR2 to immobilised peptide A4. Of these 16 peptides, only one, peptide 10, displayed the ability to inhibit AGR2–peptide A4 binding, indicating that it is this region of AGR2 (Ala108-Glu122) that PTTIYY must bind to (Figure 4b and c).

Interestingly, a recent report has also highlighted this same region of AGR2 as being important for protein–protein recognition and binding a known protein partner [50]. AGR2 has been shown to bind the ATP-binding protein reptin in vivo, and the binding interface has been pinpointed to the region between F111 to Y118 in the AGR2 primary sequence. This region is thought to represent a divergent loop in the AGR2 family of proteins and has tentatively been ascribed as a protein docking motif [50]. Our results add weight to this proposed function of this region of AGR2.

Conclusion

Here we demonstrate the feasibility of using ECD to cleave a protein's backbone whilst retaining noncovalent protein–peptide interactions. We report the fragmentation of the p53 inhibitor protein AGR2 (182AA) in complex with the PTTIYY hexapeptide. We were able to assign 18 ECD ions as AGR2 fragments, which retained the PTTIYY binding partner. Thus, we were able to directly locate the binding interface to within a 64 amino acid stretch of the AGR2 protein. This is the first successful study to analyze a noncovalent protein–peptide interaction and highlights the potential of applying this methodology for the investigation of protein–protein interfaces. Indeed, the interrogation of a protein–protein complex by ECD has very recently been described [51]. In this study, on the 147 kDa alcohol dehydrogenase tetramer, ECD produced a series of *c*-type ions that were sufficient to identify the protein using a sequence tag approach. No ECD ions could be assigned to fragments that retained the protein–protein interface. However, as the assigned fragments were located exclusively in the N-terminus of the protein, the authors could infer that the protein–protein interface is distant from this region.

From the data presented here and other recent studies highlighted above, it is clear that top-down ECD fragmentation has the potential to be a powerful technique in characterizing protein–peptide and protein–protein interactions. Future work will concentrate on applying ECD to the analysis of other biologically significant protein–peptide and developing the technique to ultimately analyze protein–protein interactions.

Acknowledgments

The authors acknowledge support for this work by the RC-UK Interdisciplinary Research Collaboration in Proteomic Technologies: RASOR consortium (BB/C511599/1). The authors thank Jenna Scotcher for help with the production of figures. The also thank Professor Neil Kelleher for the use of Prosight-PTM software.

References

1. Loo, J.A.: Studying Noncovalent Complexes by Electrospray Ionization Mass Spectrometry. *Mass Spectrom. Rev.* **16**, 1–23 (1997)
2. Ganem, B., Henion, J.D.: Going Gently into Flight: Analyzing Noncovalent Interactions by Mass Spectrometry. *Bioorg. Med. Chem.* **11**, 311–314 (2003)
3. van den Heuvel, R.H., Heck, A.J.: Native Protein Mass Spectrometry: from Intact Oligomers to Functional Machineries. *Curr. Opin. Chem. Biol.* **8**, 519–526 (2004)
4. Wyttenbach, T., Bowers, M.T.: Intermolecular Interactions in Biomolecular Systems Examined by Mass Spectrometry. *Annu. Rev. Phys. Chem.* **58**, 511–533 (2007)
5. McCullough, B.J., Gaskell, S.J.: Using Electrospray Ionization Mass Spectrometry to Study Noncovalent Interactions. *Comb. Chem. High Throughput Screen.* **12**, 203–211 (2009)
6. Breuker, K.: The Study of Protein–ligand Interactions by Mass Spectrometry—A Personal View. *Int. J. Mass Spectrom.* **239**, 33–41 (2004)
7. Schermann, S.M., Simmons, D.A., Konermann, L.: Mass Spectrometry-based Approaches to Protein–ligand Interactions. *Expert Rev. Proteom.* **2**, 475–485 (2005)
8. Hernandez, H., Robinson, C.V.: Determining the Stoichiometry and Interactions of Macromolecular Assemblies from Mass Spectrometry. *Nat. Protoc.* **2**, 715–726 (2007)
9. Zhou, M., Robinson, C.V.: When Proteomics Meets Structural Biology. *Trends Biochem. Sci.* **35**, 522–529 (2010)

10. Sharon, M., Robinson, C.V.: The Role of Mass Spectrometry in Structure Elucidation of Dynamic Protein Complexes. *Annu. Rev. Biochem.* **76**, 167–193 (2007)
11. Heck, A.J., Van Den Heuvel, R.H.: Investigation of Intact Protein Complexes by Mass Spectrometry. *Mass Spectrom. Rev.* **23**, 368–389 (2004)
12. Heck, A.J.: Native Mass Spectrometry: A Bridge Between Interactomics and Structural Biology. *Nat. Methods* **5**, 927–933 (2008)
13. Sannes-lowery, K.A., Griffey, R.H., Hofstadler, S.A.: Measuring Dissociation Constants of RNA and Aminoglycoside Antibiotics by Electrospray Ionization Mass Spectrometry. *Anal. Biochem.* **280**, 264–271 (2000)
14. Daniel, J.M., Friess, S.D., Rajagopalan, S., Wendt, S., Zenobi, R.: Quantitative Determination of Noncovalent Binding Interactions using Soft Ionization Mass Spectrometry. *Int. J. Mass Spectrom.* **216**, 1–27 (2002)
15. El-Hawiet, A., Kitova, E.N., Liu, L., Klassen, J.S.: Quantifying Labile Protein–ligand Interactions using Electrospray Ionization Mass Spectrometry. *J. Am. Soc. Mass Spectrom.* **21**, 1893–1899 (2010)
16. McLafferty, F.W., Fridriksson, E.K., Horn, D.M., Lewis, M.A., Zubarev, R.A.: Techview: Biochemistry. Biomolecule Mass Spectrometry. *Science* **284**, 1289–1290 (1999)
17. Bogdanov, B., Smith, R.D.: Proteomics by FTICR Mass Spectrometry: Top-down and Bottom-up. *Mass Spectrom. Rev.* **24**, 168–200 (2005)
18. Meng, F., Forbes, A.J., Miller, L.M., Kelleher, N.L.: Detection and Localization of Protein Modifications by High Resolution Tandem Mass Spectrometry. *Mass Spectrom. Rev.* **24**, 126–134 (2005)
19. Siuti, N., Kelleher, N.L.: Decoding Protein Modifications using Top-down Mass Sspectrometry. *Nat. Methods* **4**, 817–821 (2007)
20. Zubarev, R.A., Kelleher, N.L., McLafferty, F.W.: Electron Capture Dissociation of Multiply Charged Protein Cations. A Nonergodic Process. *J. Am. Chem. Soc.* **120**, 3265–3266 (1998)
21. Zubarev, R.A., Horn, D.M., Fridriksson, E.K., Kelleher, N.L., Kruger, N.A., Lewis, M.A., Carpenter, B.K., McLafferty, F.W.: Electron Capture Dissociation for Structural Characterization of Multiply Charged Protein Cations. *Anal. Chem.* **72**, 563–573 (2000)
22. Cooper, H.J., Hakansson, K., Marshall, A.G.: The Role of Electron Capture Dissociation in Biomolecular Analysis. *Mass Spectrom. Rev.* **24**, 201–222 (2005)
23. Haselmann, K.F., Jorgensen, T.J., Budnik, B.A., Jensen, F., Zubarev, R. A.: Electron Capture Dissociation of Weakly Bound Polypeptide Polycationic Complexes. *Rapid Commun. Mass Spectrom.* **16**, 2260–2265 (2002)
24. Xie, Y., Zhang, J., Yin, S., Loo, J.A.: Top-down ESI-ECD-FTICR Mass Spectrometry Localizes Noncovalent Protein–ligand Binding Sites. *J. Am. Chem. Soc.* **128**, 14432–14433 (2006)
25. Yin, S., Loo, J.A.: Elucidating the Site of Protein-atp Binding by Top-down Mass Spectrometry. *J. Am. Soc. Mass Spectrom.* **21**, 899–907 (2010)
26. Yin, S., Loo, J.A.: Top-down Mass Spectrometry of Supercharged Native Protein–ligand Complexes. *Int. J. Mass Spectrom.* **300**, 118–122 (2010)
27. Yin, S., Xie, Y., Loo, J.A.: Mass Spectrometry of Protein–ligand Complexes: Enhanced Gas-phase Stability of Ribonuclease–nucleotide Complexes. *J. Am. Soc. Mass Spectrom.* **19**, 1199–1208 (2008)
28. Liu, L., Bagal, D., Kitova, E.N., Schnier, P.D., Klassen, J.S.: Hydrophobic Protein–ligand Interactions Preserved in the Gas Phase. *J. Am. Chem. Soc.* **131**, 15980–15981 (2009)
29. Horn, D.M., Ge, Y., McLafferty, F.W.: Activated Ion Electron Capture Dissociation for Mass Spectral Sequencing of Larger (42 kDa) Proteins. *Anal. Chem.* **72**, 4778–4784 (2000)
30. Hakansson, K., Chalmers, M.J., Quinn, J.P., McFarland, M.A., Hendrickson, C.L., Marshall, A.G.: Combined electron capture and infrared multiphoton dissociation for multistage MS/MS in a fourier transform ion cyclotron resonance mass spectrometer. *Anal. Chem.* **75**, 3256–3262 (2003)
31. Tsybin, Y.O., Witt, M., Baykut, G., Kjeldsen, F., Hakansson, P.: Combined Infrared Multiphoton Dissociation and Electron Capture Dissociation with a Hollow Electron Beam in Fourier Transform Ion Cyclotron Resonance Mass Spectrometry. *Rapid Commun. Mass Spectrom.* **17**, 1759–1768 (2003)
32. Wang, Z., Hao, Y., Lowe, A.W.: The Adenocarcinoma-associated Antigen, AGR2, Promotes Tumor Growth, Cell Migration, and Cellular Transformation. *Cancer Res.* **68**, 492–497 (2008)
33. Brychtova, V., Vojtesek, B., Hrstka, R.: Anterior Gradient 2 a Novel Player in Tumor Cell Biology. *Cancer Lett.* **304**, 1–7 (2011)
34. Mackay, A., Urruticoechea, A., Dixon, J.M., Dexter, T., Fenwick, K., Ashworth, A., Drury, S., Larionov, A., Young, O., White, S., Miller, W. R., Evans, D.B., Dowsett, M.: Molecular Response to Aromatase Inhibitor Treatment in Primary Breast Cancer. *Breast Cancer Res.* **9**, R37 (2007)
35. Hrstka, R., Nenutil, R., Fourtouna, A., Maslon, M.M., Naughton, C., Langdon, S., Murray, E., Larionov, A., Petrakova, K., Muller, P., Dixon, M.J., Hupp, T.R., Vojtesek, B.: The Pro-metastatic Protein Anterior Gradient-2 Predicts Poor Prognosis in Tamoxifen-treated Breast Cancers. *Oncogene* **29**, 4838–4847 (2010)
36. Zhang, Y., Forootan, S.S., Liu, D., Barraclough, R., Foster, C.S., Rudland, P.S., Ke, Y.: Increased Expression of Anterior Gradient-2 is Significantly Associated with Poor Survival of Prostate Cancer Patients. *Prostate Cancer Prostatic Dis.* **10**, 293–300 (2007)
37. Zweitzig, D.R., Smirnov, D.A., Connelly, M.C., Terstappen, L.W., O'Hara, S.M., Moran, E.: Physiological Stress Induces the Metastasis Marker AGR2 in Breast Cancer Cells. *Mol. Cell. Biochem.* **306**, 255–260 (2007)
38. Pohler, E., Craig, A.L., Cotton, J., Lawrie, L., Dillon, J.F., Ross, P., Kernohan, N., Hupp, T.R.: The Barrett's Antigen Anterior Gradient-2 Silences the p53 Transcriptional Response to DNA Damage. *Mol. Cell. Proteom.* **3**, 534–547 (2004)
39. Ramachandran, V., Arumugam, T., Wang, H., Logsdon, C.D.: Anterior Gradient 2 is Expressed and Secreted During the Development of Pancreatic Cancer and Promotes Cancer Cell Survival. *Cancer Res.* **68**, 7811–7818 (2008)
40. Fourtouna, A., Murray, E., Nicholson, J., Maslon, M.M., Pang, L., Dryden, D.T.F., Hupp, T.R.: The Anterior Gradient-2 Pathway as a Model for Developing Peptide-aptamer Anti-cancer Drug Leads that Stimulate p53 Function. *Curr. Chem. Biol.* **3**, 124–137 (2009)
41. Clarke, D.J., Stokes, A.A., Langridge-Smith, P., Mackay, C.L.: Online Quench-flow Electrospray Ionization Fourier Transform Ion Cyclotron Resonance Mass Spectrometry for Elucidating Kinetic and Chemical Enzymatic Reaction Mechanisms. *Anal. Chem.* **82**, 1897–1904 (2010)
42. LeDuc, R.D., Kelleher, N.L.: Using Prosight PTM and Related Tools for Targeted Protein Identification and Characterization with High Mass Accuracy Tandem MS Data. *Curr. Protoc. Bioinformatics* Unit 13 6, Chapter 13 (2007)
43. Murray, E., McKenna, E.O., Burch, L.R., Dillon, J., Langridge-Smith, P., Kolch, W., Pitt, A., Hupp, T.R.: Microarray-formatted Clinical Biomarker Assay Development Using Peptide Aptamers to Anterior Gradient-2. *Biochemistry* **46**, 13742–13751 (2007)
44. Frimpong, A.K., Abzalimov, R.R., Uversky, V.N., Kaltashov, I.A.: Characterization of Intrinsically Disordered Proteins with Electrospray Ionization Mass Spectrometry: Conformational Heterogeneity of ↦-Synuclein. *Proteins* **78**, 714–722 (2010)
45. Konermann, L., Douglas, D.J.: Equilibrium Unfolding of Proteins Monitored by Electrospray Ionization Mass Spectrometry: Distinguishing Two-state from Multi-state Transitions. *Rapid Commun. Mass Spectrom.* **12**, 435–442 (1998)
46. Konermann, L., Rosell, F.I., Mauk, A.G., Douglas, D.J.: Acid-induced Denaturation of Myoglobin Studied by Time-resolved Electrospray Ionization Mass Spectrometry. *Biochemistry* **36**, 6448–6454 (1997)
47. Breuker, K., Bruschweiler, S., Tollinger, M.: Electrostatic Stabilization of a Native Protein Structure in the Gas Phase. *Angew. Chem. Int. Ed. Engl.* **50**, 873–877 (2011)
48. Sterling, H.J., Williams, E.R.: Origin of Supercharging in Electrospray Ionization of Noncovalent Complexes from Aqueous Solution. *J. Am. Soc. Mass Spectrom.* **20**, 1933–1943 (2009)
49. Sterling, H.J., Daly, M.P., Feld, G.K., Thoren, K.L., Kintzer, A.F., Krantz, B.A., Williams, E.R.: Effects of Supercharging Reagents on Noncovalent Complex Structure in Electrospray Ionization from Aqueous Solutions. *J. Am. Soc. Mass Spectrom.* **21**, 1762–1774 (2010)
50. Maslon, M.M., Hrstka, R., Vojtesek, B., Hupp, T.R.: A Divergent Substrate-binding Loop within the Pro-oncogenic Protein Anterior gGradient-2 forms a Docking Site for Reptin. *J. Mol. Biol.* **404**, 418–438 (2010)
51. Zhang, H., Cui, W., Wen, J., Blankenship, R.E., Gross, M.L.: Native Electrospray and Electron-capture Dissociation in FTICR Mass Spectrometry Provide Top-down Sequencing of a Protein Component in an Intact Protein Assembly. *J. Am. Soc. Mass Spectrom.* **21**, 1966–1968 (2010)